Assimilation of lidar back-scatter and wind retrievals of planetary boundary layer height into WRF atmospheric forecast states.

Andrew Tangborn[1], Belay Demoz[1,2], Brian J. Carroll[2], Joseph Santanello[3]and Jeffrey L. Anderson[4]

[1]JCET, UMBC, Baltimore, MD, USA
[2]Dept. of Physics, UMBC, Baltimore, MD, USA
[3]Laboratory for Hydrology, NASA GSFC, Greenbelt, MD, USA
[4]National Center for Atmospheric Research, Boulder, CO, USA

Key Points:

- An ensemble based data assimilation system has been developed to determine covariances between PBLH and atmospheric state variables.
- Ground based PBLH measurements are shown to improve model estimates of temperature, moisture and velocity relative to independent data.
- The largest improvements were in the late afternoon during growth of the convective layer.

Corresponding author: Andrew Tangborn, tangborn@umbc.edu

Abstract

Lidar backscatter and wind retrievals of the planetary boundary layer height (PBLH) are assimilated into forecasts from the NASA Unified - Weather and Research Forecast (NU-WRF) model during the Plains Elevated Convection Convection at Night (PECAN) campaign on July 11, 2015 in Greensburg, Kansas, using error statistics collected from the model profiles to compute the necessary covariance matrices. Assimilation of the observed PBLH was found to improve the temperature, water vapor and velocity profiles relative to independent sonde profiles in the late afternoon, while little improvement was seen during the night and early morning. The computed forecast error covariances between the PBLH and state variables were found to rise in the late afternoon, leading to the larger improvements at this time.

1 Plain Language Summary

Computer models of the Earth's atmosphere have difficulty to accurately predict the height of the planetary boundary layer (PBL), which is the lowest layer of the atmosphere and that which exchanges energy and moisture with the Earth's surface. Accurate prediction of the PBL layer is essential to both numerical weather prediction (NWP) and pollution forecasting. PBL height (PBLH) observations are difficult to combine with these models because it is not a predictive variable, meaning that it doesn't influence future atmospheric changes in the models. This paper presents a methodology to combine these measurements with the models through a statistical data assimilation approach that calculates the correlation between the PBLH and variables like temperature and moisture in the model. We show that the model estimates of these variables can be improved via this method, and this will enable increased model accuracy.

2 Introduction

The planetary boundary layer (PBL) plays an important role in both weather and climate. This layer is where the Earth's surface interacts with the atmosphere, exchanging heat, moisture and pollutants. The PBL height (PBLH) is central to these interactions and is controlled by the energy flux from the surface. Under certain conditions during daytime it defines the convective boundary layer (CBL) and during nighttime it is the stable (non-convective) boundary layer (SBL). Trace gases and aerosols emitted from the surface are rapidly transported within this layer by turbulent atmospheric motion, and transfer of energy and mass into the free troposphere occurs across an interfacial layer at the top of the PBL. The PBLH is fundamental to weather, climate, atmospheric turbulence and pollution through its role in land-atmosphere interactions and mediation of Earth's water and energy cycles (Santanello et al. 2018) and its impact on convection in the troposphere, which is generally initiated within the boundary layer and then penetrates the top (Hong and Pan, 1998; Browning, et al. 2007). Thus, accurate knowledge of the PBLH is essential for both weather and climate forecasting.

The PBLH is defined by thermodynamic properties such as a temperature inversion or hydrolapse which can be measured by radiosonde. Alternatively the drop off in aerosol concentration that occurs across the top of the PBL is used, since aerosols are well mixed throughout the PBL (Hicks, et al., 2019). Atmospheric models rely on parameterization schemes to define the structure of the PBL and compute PBLH. These are generally either local mixing schemes that use local turbulent kinetic energy (TKE, Janjic, 1994) or flux schemes (Hong and Pan, 1996). Generally, these PBL parameterizations have systematically higher PBLH relative to observed values (Hegarty et al., 2018), and also have difficulties modeling the growth of the convective layer during the morning. These varying and distinct definitions of PBLH across models and observations re-

main a challenge in terms of utilizing both for process understanding or model evaluation/development.

Observations of PBLH are traditionally made by radiosonde measurements, which have high vertical resolution but are expensive to launch frequently and are thus limited to special experiments and/or ill-timed launches (*e.g.* 00/12Z National Weather Service launches) with respect to the convective and stable PBL development. Likewise, spaceborne measurements of the lower troposphere from passive and active instruments (with the exception of Global Positioning System Radio Occultation (GPSRO), Ao, et al. 2008) are severely limited in vertical, spatial, and/or temporal resolution (Wulfmeyer et al. 2015). Ground based measurement of PBLH has been proposed for an extensive network of ceilometers by adding to the functionality of instruments that were designed for measuring cloud heights [Hicks et al., 2016]. The ceilometer measures the time required for a laser pulse to return to a receiver, from which the height of the scattering is determined. The intensity of the backscatter is correlated with the density of aerosols at a given height and the PBLH is inferred from the location of the maximum negative gradient of the backscatter intensity. Several algorithms employ wavelet transforms to identify the location of the negative gradient (e.g. Brooks, 2003; Knepp, *et al.*, 2017), which relies on finding the wavelet dilation that is large enough to be distinct from noise and small-scale gradients in the backscatter profile. This existing network of ceilometers could be used to create a relatively dense network of frequent PBLH observations, as was recommended by the 2009 study from the National Research Council (NRC, 2009) and the Thermodynamic Profiling Technologies Workshop (NCAR, 2012). Doppler lidar is a more complex type of lidar than a ceilometer, reporting aerosol-correlated backscatter like a ceilometer but also wind speed profiles. This allows incorporation of wind variance into PBLH measurement (e.g., Tucker et al. 2009). Wind variance is indicative of turbulent mixing such as that found in the convective PBLH.

The question remaining is how to assimilate these observations into a numerical weather prediction (NWP) model? PBLH is a diagnostic variable in NWP parameterized physics models. This means any correction to PBLH will be lost during the model forecast unless the PBLH height observation is used to correct state variables such as temperature and moisture. This could be done either by creating an adjoint of the PBL parameterization scheme, or through the use of an ensemble Kalman filter which would determine the error covariances between PBLH and state variables in the model. The structure of the covariance, and how the state variables are changed by assimilating PBLH, will depend on which PBL scheme is used. We will show how such a system could work by conducting a posteriori lidar PBLH observation impact experiments using forecast fields from a NASA Unified - Weather and Research Forecast (NU-WRF, Lidard-Peters, 2015) model run for one day during the Plains Elevated Convection at Night (PECAN) campaign on July 11, 2015. The assimilation is done on hourly WRF forecast fields throughout the day without cycling the analysis fields back into the model. In this paper, we demonstrate a new and promising method that uses the relative lidar-based aerosol backscatter and wind derived PBLH to correct model forecasted state variables.

3 Methodology

The assimilation methodology is based on the ensemble Kalman filter (EnKF)(Evensen, 2009), where the analysis state is the estimate with the minimum estimated errors, relative to the given error statistics. It differs from the EnKF in that the analysis is not used as an initial state for the next model forecast. Rather, two existing one day NU-WRF forecasts, with different PBL physics schemes, are used when lidar measurements are available at a single location. And as a proxy for an ensemble of forecasts, we use profiles from neighboring model gridpoints to obtain and estimate of error statistics. This approach will only allow for the construction of the vertical component of covariance, but this is the component that we need in order to understand how PBLH can be used

to correct atmospheric profiles through the use of profile and PBLH statistics. We use profiles from the entire 220 × 220 model grid (and thus an ensemble of 48,400) which includes profiles far from the analysis location. An ensemble Kalman filter would likely give different covariance information, but the basic relationship between the state variable profiles and the PBLH are determined by the model in the same manner here. This approach is similar to Ensemble Optimal Interpolation (EnOI), developed for ocean data assimilation (Oke, *et al.*, 2010).

The two NU-WRF simulations use the Mellor–Yamada–Janjic (MYJ)[Mellor and Yamada, 1974, 1982; Janjic, 2002] and Mellor-Yamada-Nakanishi-Niino level 2.5 (MYNN) [Nakanishi and Niino, 2009] which are local 1.5 and 2.5 order turbulence closure schemes respectively. The NU-WRF forecast state variables are temperature (T), moisture (Q) and velocity (U,V), and we define the forecast vector $\mathbf{x}^f = [T^f\ Q^f\ U^f\ V^f\ (PBLH)^f]$, where we have combined PBLH with the state variables to enable the covariance calculation between them.

The forecast error covariance, $\mathbf{P}^f$ is defined as

$$\mathbf{P}^f = \left\langle (\mathbf{x}^f - \mathbf{x}^t)(\mathbf{x}^f - \mathbf{x}^t)^T \right\rangle \tag{1}$$

where the summation is over the grid points $i = 1, N_{lon}$, $j = 1, N_{lat}$ and $\mathbf{x}^t$ is the (unknown) true state, on the discrete model grid. We only assimilate the observation $y^o = PBLH = H(\mathbf{x}^f)$ where H is the non-linear observation operator. The analysis equation is

$$\mathbf{x}^a = \mathbf{x}^f + \mathbf{K}(y^o - H(\mathbf{x}^f)) \tag{2}$$

where the gain matrix, $\mathbf{K}$ is defined by:

$$\mathbf{K} = \mathbf{P}^f\mathbf{H}^T(\mathbf{H}\mathbf{P}^f\mathbf{H}^T + (\sigma^o)^2)^{-1}, \tag{3}$$

σ^o is the observation error standard deviation supplied with the lidar retrievals, and $\mathbf{H}$ is the linearized observation operator for PBLH. Because the PBLH is related to the state variables via the two PBL physics schemes, determining $\mathbf{H}$ would require linearizing the PBL physics at every analysis time. Instead of this approach, we use the ensemble of profiles from the forecast field locations $\mathbf{x}^f$ and the boundary layer heights $PBLH^f$ to obtain the ensemble estimates:

$$\mathbf{P}^f\mathbf{H}^T \approx \left\langle (\mathbf{x}^f - {\mu_\mathbf{x}}^f)\ (H(\mathbf{x}^f - {\mu_\mathbf{x}}^f))^T \right\rangle \tag{4}$$

and

$$\mathbf{H}\mathbf{P}^f\mathbf{H}^T \approx \left\langle H(\mathbf{x}^f - {\mu_\mathbf{x}}^f)\ (H(\mathbf{x}^f - {\mu_\mathbf{x}}^f))^T \right\rangle \tag{5}$$

where ${\mu_\mathbf{x}}^f$ is the mean forecast state of the ensemble of profiles.

We expect the correlation between the airmass within the PBL and the free troposphere to drop away rapidly, because of limited intereactions between them. We found that this can cause errors in the analysis profiles if error covariance and PBLH is allowed to continue into the troposphere. To reduce these errors we have added an exponential decay starting at the model level closest to the PBLH (k_{PBLH}) to define a vertical localization factor:

$$C_{loc} = exp\left[-\alpha(\frac{k - k_{PBLH}}{k_{PBLH}})^2\right] \tag{6}$$

where k is the model level and α is an experimentally determined factor. This ensures that the covariance between the PBLH and the state variables becomes small within a couple of model levels into the free troposphere.

This system is solved each time that lidar profile observations are available, and the resulting analysis fields are compared to sonde profiles when the latter are also available. We focus on the impact of the assimilation on the state variables T, Q, U and V rather than the PBLH because only the state variables would be retained by a forecast.

4 Results

The NU-WRF simulations, taken from existing forecast runs used for the PECAN campaign (Santanello *et al.*, 2019) are initialized using a National Center for Environmental Prediction (NCEP) Global Forecast System (GFS) reanalysis interpolated to the domain 30-48N and 84-110 W, with 54 vertical levels. The two forecast runs were conducted using MYJ PBL physics (2-22 UTC) and MYNN (2-23 UTC) on July 11, 2015. Lidar PBLH observations were made every 25 minutes on that day in Greensburg, KS (37.6 N, 99.3 W), while balloon soundings were launched from that location 6 times as part of the Plains Elevated Convection At Night (PECAN; Gerts et al. 2017). Figure 1 shows the PBLH during that day and derived from the two NU-WRF forecasts, lidar observations and soundings. We have determined the sounding PBLH using the parcel method, which defines the top as the height where the potential temperature first exceeds the ground temperature. The lidar PBLH (black *, derived using the method reported in Bonin, 2018) closely matches the sonde estimates (green triangles) in the late evening to early morning (2-7 UTC), while it is somewhat lower in the afternoon. The two NU-WRF forecasts differ from the observations depending on the time of day. In the early morning and early afternoon the MYJ forecasts (red triangles) are slightly higher than the observations, then fall behind the rise seen in the lidar observations (there are no sonde measurements to compare to here) before rising much higher than the observations in the late afternoon. The MYNN forecasts (blue squares) are lower than the observations from early morning until early afternoon before rising higher (but not as high as MYJ).

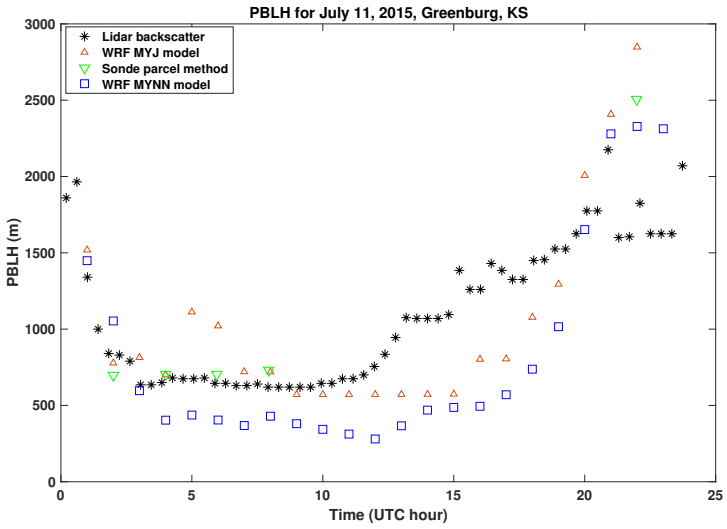

c

Figure 1. PBLH vs UTC time for July 11, 2015 for lidar backscatter (black *), WRF model - MYJ (red triangles), sonde observations using parcel method (green triangles) and WRF model - MYNN (blue squares).

Since we are primarily interested in the impact of the assimilation on state variables within the boundary layer, in Figure 2 we plot the RMS difference between the model and the independent (unassimilated) sonde profiles from the surface to roughly the top of the boundary layer (first 8 levels, or about 800 mb). So for the temperature forecast,

the RMS difference would be

$$RMS(t_a) = \left[\frac{1}{8}\sum_{i=1}^{8}(T_i^f - T_i^{sonde})^2\right]^{1/2} \quad (7)$$

where t_a is the analysis time and *ntop* is the model level at the top of the PBL. Figure 2 shows the RMS differences with the sonde profiles throughout the day for the forecasts (blue) and analyses (red) for potential temperature (a), water vapor mixing ratio (b) and the U (c) and V (d) components of velocity. The MYNN profiles are shown by solid lines while the MYJ profiles are dashed lines. During the night (2-9 UTC), the assimilation has very little impact on the potential temperature RMS differences in the early morning (6 and 8 UTC), and the two forecasts have similar accuracy. By late afternoon (22 and 23 UTC, note that the MYJ forecast stops at 22 UTC) the sonde comparisons show that the assimilation reduces RMS differences in the potential temperatures by nearly 50% for MYNN and around 80% for MYJ. The water vapor mixing ratio (b) also has little impact from the assimilation until 22 UTC, and then the RMS difference for the MYJ analysis more than doubles whereas it decreases by roughly half for MYNN. The forecasts for the 2 schemes show about the same differences with the sonde moisture profiles throughout the day. The U-velocity profiles (c) begin to show differences between the MYJ and MYNN by 8 UTC (3 a.m. local time) and the assimilation reduces the RMS differences with sonde profiles significantly by 22 UTC for both models. The V-velocity profiles (d) begin to differ between MYJ and MYNN for the forecasts at 8 UTC, and assimilation reduces the RMS differences with sondes in late afternoon by 10-20%.

To better understand these comparisons with sonde profiles, we focus on the profile details at 22 UTC for each of the state variables for the MYJ model. Figure 3 shows the potential temperature (a), water vapor mixing ratio (b), u-velocity (zonal) (c) and v-velocity (meridional) (d) for the sonde (green), forecast (blue) and analysis (red). The assimilation of the lidar PBLH measurement is seen to reduce the temperature within the PBL, drawing it closer to the independent (unassimilated) sonde profile. Initial experiments without vertical covariance localization (not shown) found that the analysis profiles were changed substantially well into the troposphere, which increased the RMS differences with the sonde profiles there. With the addition of the vertical correlation the analysis profiles relax back to the forecast in the troposphere. The WV profile is shown to be increased by the assimilation (since WV and PBLH are negatively correlated and higher PBLH corresponds to lower WV levels in the PBL models), but the analysis overshoots the sonde WV profile, hence causing the increase in the RMS difference in Figure 2(b). Compared to temperature, WV is highly variable in time and space and it has been shown in the past that slanted balloon trajectories under estimate the WV present (Demoz et al 2006; Crook, 1996). The PBLH may be a macroscale observation that is forcing a correction to the WV flux and hence pointing out an issue in measurements. Future studies should look at the profile measurements of WV from lidars. The two components of velocity (c,d) are both drawn towards the sonde profiles, but by more modest amounts. These analysis profiles in show that, for this one analysis time, the assimilation is pushing the state variables in the proper direction. The reason for these corrections to the state variable profiles is that the error covariance between PBLH and each state variable, $\mathbf{P}^f\mathbf{H}^T$, can be computed from the ensemble of profiles that was collected from the model grid. The forecast PBLH for each profile was computed using the full PBL physics, and therefore contains the essential correlation information between these variables.

We can understand why the assimilation did not result in any significant corrections to the state profiles until late afternoon by plotting the error covariance between PBLH and each of the state variables, seen in Figure 4 at different times during the day.

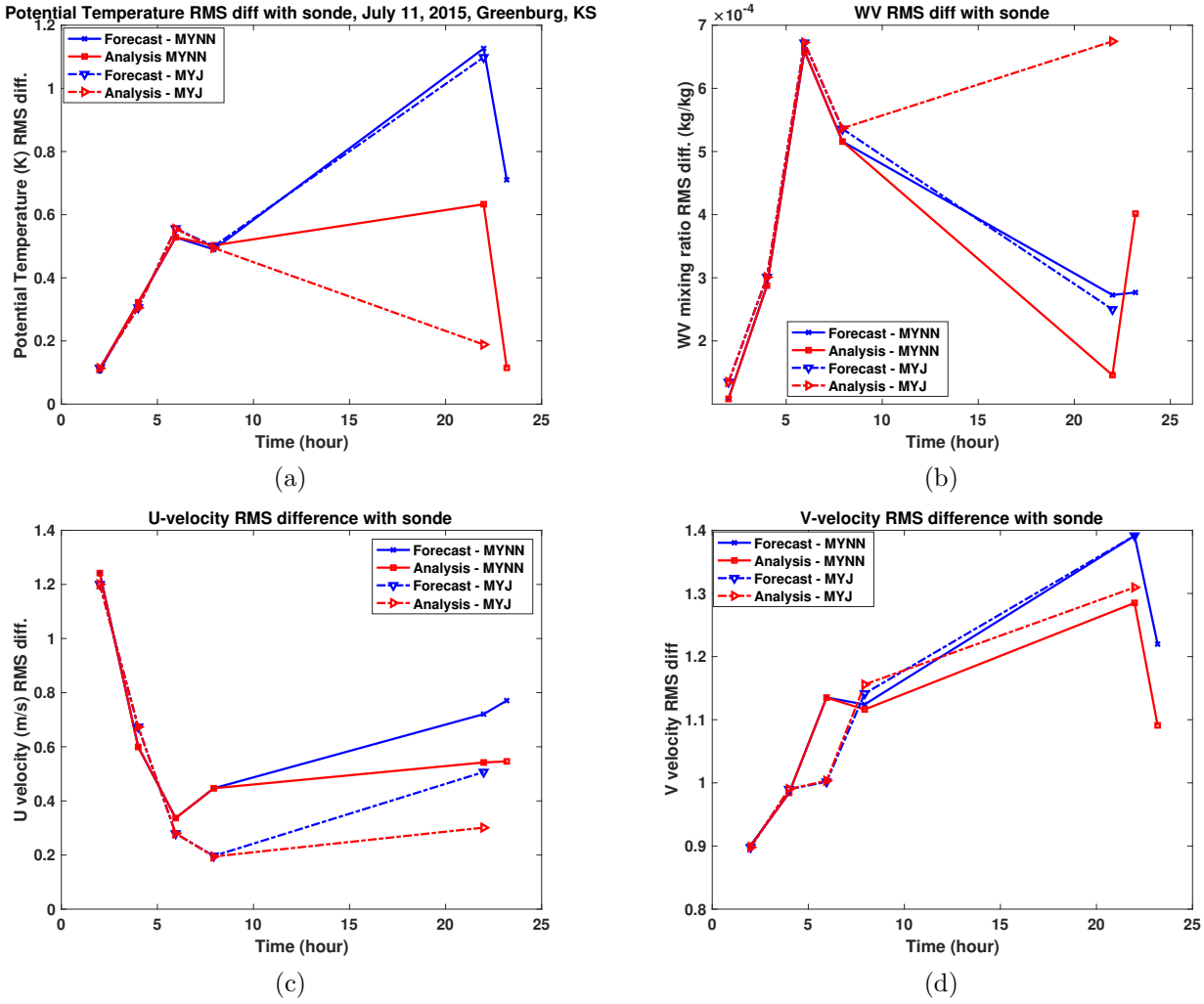

Figure 2. RMS difference from surface to top of PBL vs. time of forecast (blue) and analysis (red) with sonde profiles for (a) potential temperature, (b) water vapor, (c) zonal velocity and (d) meridional velocity. The solid lines are for the MYNN PBL model and the dashed lines are for the MYJ PBL model.

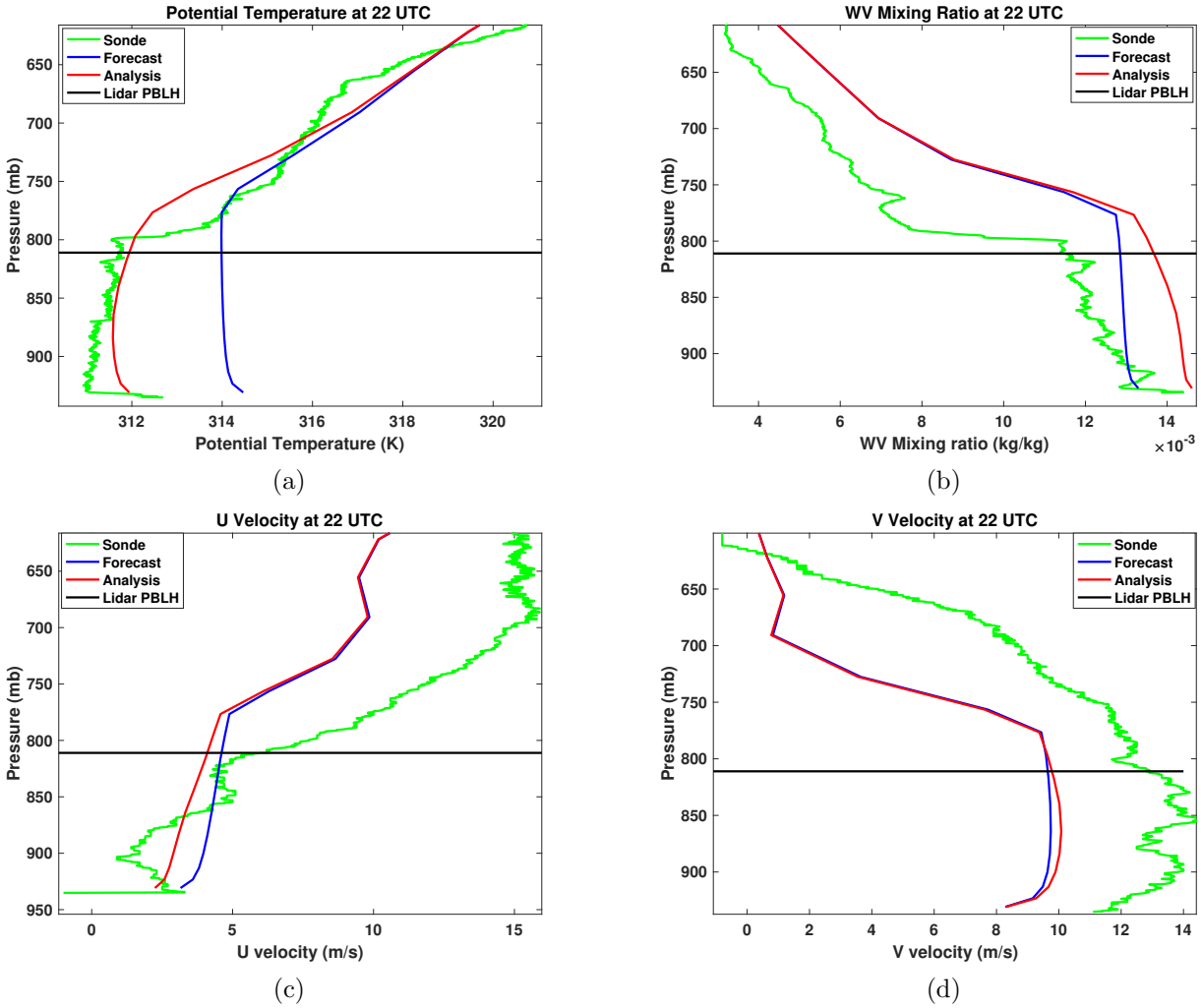

Figure 3. Profiles from sonde (green), forecast (blue) and analysis (red) for potential temperature (a), water vapor mixing ratio (b), u-velocity (c) and v-velocity (d) at 22 UTC, July 11, 2015 in Greensburg, KS. The lidar measurement of the PBL height is given by the horizontal black line. The model uses the MYJ physics for these profiles.

The covariance with temperature (a) is always positive, and grows by a factor of 4 by late afternoon near the surface. The covariance with WV is mostly negative and grows by roughly a factor of 5, while the covariance with the two components of velocity oscillate between positive and negative and shows less consistent growth. Thus, the most significant impact of assimilation to temperature and moisture occur in late afternoon while more limited velocity corrections are largely constrained by the correlations determined by the ensemble of model forecast states.

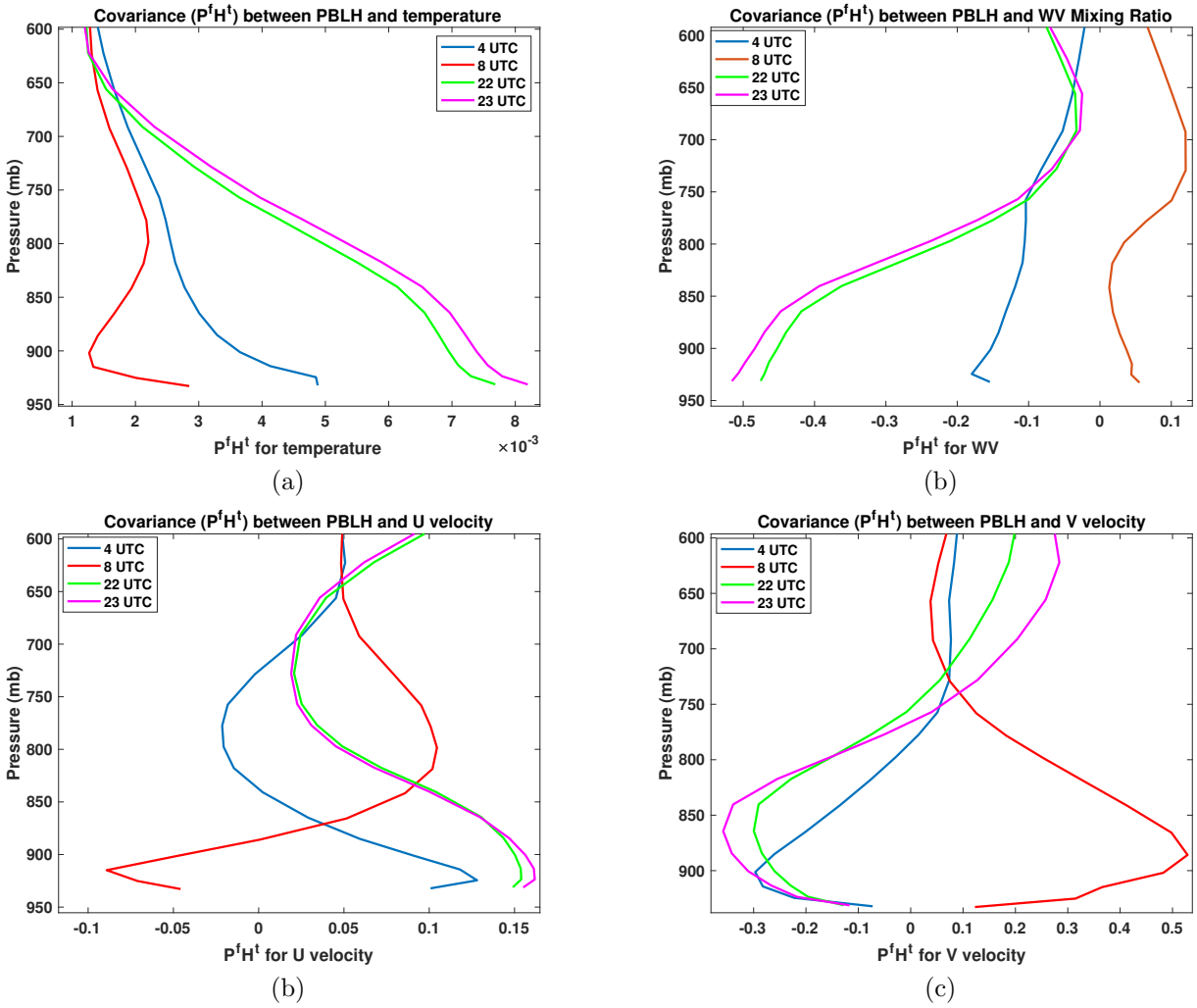

Figure 4. Covariance $\mathbf{P}^f\mathbf{H}^T$ between PBLH and temperature (a), water vapor (b), U-velocity (c) and V-velocity (d), at times 4, 8, 22 and 23 UTC, for PBL physics model MYHH.

5 Conclusions

These offline data assimilation experiments indicate that assimilation ground based lidar backscatter and wind measurements of PBLH into a regional NWP model will likely lead to significant improvements within the PBL, particulary when this approach is applied to an EnKF assimilation system with cycling. Using two NU-WRF forecasts over a period of one day with different PBL physics models, we show how the state variables, T, WV, U and V can be corrected using an an assimilation system with ensemble based error covariances. During the night and early morning the assimilation has little or no

impact on the state variables, but by late afternoon the temperature field is drawn closer to independent sonde measurements. The water vapor mixing ratio is over corrected in the direction of sonde data, and this could likely be tuned in an assimilation system. The assimilation corrected the two velocity components by smaller amounts, but still reduced differences with the sonde profiles. These corrections are the result of ensemble computed error covariances between the PBLH and the state variable profiles within the PBL. The results here indicate that this approach could be used in a forecast system in a way that that the PBLH observational information could be carried forward in time so as to improve the forecast accuracy within the PBL.

This work is intended only to demonstrate a necessary first step in terms of how ensemble statistics can help to constrain profiles within the PBL by assimilating PBLH observations. A more complete demonstration of this approach will require the construction of an EnKF, and run over many days with a variety of weather patterns, including significantly warmer(cooler) and wetter(drier) days. And the vertical localization employed here will likely need to be further refined, to account for the variability of the PBL growth each day, and how the physical process of entrainment interacts with the free troposphere. A detailed work extending this paper with multiple cases is planned and will be the subject of an extended publication elsewhere.

Acknowledgments

B. Demoz was funded by National Science Foundation award (AGS-1503563) to the University of Maryland, Baltimore County and through NOAA Cooperative Science Center in Atmospheric Sciences and Meteorology, funded by the Educational Partnership Program at NOAA in collaboration with Howard University.

PECAN (`https://data.eol.ucar.edu/master_list/?project=PECAN\verb`) data are archived by NCAR/EOL, which is funded by NSF. The forecast and analysis fields produced for this work are stored at https://alg.umbc.edu/pecan/.

6 References

Ao, C.O., T. K. Chan, B. A. Iijima, J.-L. Li, A. J. Mannucci, J. Teixeira, B. Tian, and D. E. Waliser (2008), Planetary boundary layer information from GPS radio occultation measurements, *Proceedings of GRAS SAF Workshop on Applications of GPSRO Measurements*, ECMWF, Reading, UK.

Banks, R. F., J. Tiana-Alsina, F. Rocadenbosch, and J. M. Baldasano (2015) Performance evaluation of the boundary-layer height from lidar and the Weather Research and Forecasting Model at an urban coastal site in the north-east Iberian Peninsula. *Bound.-Layer Meteor.*, 157, 265–292, https://doi.org/ 10.1007/s10546-015-0056-2.

Bonin, T.A., B.J. Carroll, R.M. Hardesty, W.A. Brewer, K. Hajney, O.E. Salmon and P.B. Shepson (2018), Doppler Lidar Observations of the Mixing Height in Indianapolis Using an Automated Composite Fuzzy Logic Approach, *J. Atmos. Ocean Tech.*, 35, 473-490.

Browning, K. A., and Coauthors (2007), The Convective Storm Initiation Project. , *Bull. Amer. Meteor. Soc.*, 88, 1939–1955, https://doi.org/10.1175/BAMS-88-12-1939.

Cohen, A.E., S.M. Cavallo, M.C. Coniglio and H.E. Brook (2015), A Review of Planetary Boundary Layer Parameterization Schemes and Their Sensitivity in Simulating Southeastern U.S. Cold Season Severe Weather Environments, *Wea. Forecat.*, 30, 591-612.

Evensen, G. (2009), *Data assimilation: the ensemble Kalman filter*, Springer.

Geerts, B., and Coauthors, (2017), The 2015 Plains Elevated Convection At Night field project. *Bull. Amer. Meteor. Soc.*, 98, 767–786, https://doi.org/10.1175/BAMS-D-15-00257.1.

Hegarty, J.D., J. Lewis, E.L. McGrath-Spangler, J. Henderson, A.J. Scarino, P. DeCola, R. Ferrare, M. Hicks, R.D. Adams-Selin and E.J. Welton (2018) Analysis of the Planetary Boundary Layer Height during DISCOVER-AQ Baltimore–Washington, D.C., with Lidar and High-Resolution WRF Modeling, *J. Appl. Meteo. Climat.*, 57, 2679-2696.

Hicks, M., D. Atkinson, B. Demoz, K. Vermeesch and R. Delgado (2016), The National Weather Service Ceilometer Planetary Boundary Layer Project, *The 27th International Laser Radar Conference (ILRC 27)*, https://doi.org/10.1051/epjconf/201611915004.

Hicks, M., B. Demoz, K. Vermeesch and D. Atkinson (2019), Intercomparison of Mixing Layer Heights from the National Weather Service Ceilometer Test Sites and Collocated Radiosondes, *J. Atmos. Ocean Tech.*, 36, 129-137.

Hong, S.-Y. and H.-L. Pan (1996), Nonlocal boundary layer vertical diffusion in a medium-range forecast model, *Mon. Wea. Rev.*, 124, 2332-2339.

Hong, S.-Y. and H.-L. Pan (1998), Convective Trigger Function for a Mass-Flux Cumulus Parameterization Scheme, *Mon. Wea. Rev*, 126, 2599-2620.

Janjic, Z.I. (1994), The Step-mountain eta coordinate model: Further developments of the convection, viscous sublayer, and turbulence closure, *Mon. Wea. Rev.*, 122, 927-945.

Janjic, Z.I. (2002), Nonsingular Implementation of the Mellor-Yamada Level 2.5 Scheme in the NCEP Meso model (NCEP Office Note No. 437).

T. N. Knepp, J.J. Szykman, R. Long, R. M. Duvall, J. Krug, M. Beaver, K. Cavender, K. Kronmiller, M. Wheeler, R. Delgado, R. Hoff, T. Berkoff, E. Olson, R. Clark, D. Wolfe, D. Van Gilst, D. Neil (2017), Assessment of mixed-layer height estimation from single-wavelength ceilometer profiles, *Atmos. Meas. Tech.*, 10, 3963-3983.

Mellor, G.L. and T. Yamada (1974), A Hierarchy of Turbulence Closure Models for Planetary Boundary Layers, *J. Atmos. Sci.*, 31, 1791-1806.

Mellor, G.L. and T. Yamada (1982), Development of a turbulence closure model for geophysical fluid problems, *Rev. Geophys.*, 20, 851-875.

Nakashini, M. and H. Niino (2009), Development of an improved turbulence closure model for the atmospheric boundary layer, *J. Met. Soc. Japan*, 87, 895-912.

National Research Council (2009), Observing Weather and Climate from the Ground Up: A Nationwide Network of Networks, in: Observing Weather and Climate from the Ground

Up: A Nationwide Network of Networks, 1–234, Natl. Academies Press, 2101 Constitution Ave, Washington, DC 20418 USA.

NCAR Technical Note (2012), Thermodynamic Profiling Technologies Workshop Report to the National Science Foundation and the National Weather Service, National Center for Atmospheric Research.

Oke, P.R., G.B. Brassington, D.A. Griffin, and A. Schiller (2010), Ocean data assimilation: a case for ensemble optimal interpolation, *Austr. Meteor.Ocean. J.*, 59, 67-76.

Peters-Lidard, C.A. and Co-authors (2015), Integrated modeling of aerosol, cloud, precipitation and land processes at satellite-resolved scales, *Environ. Mod. Soft.*, 67, 149-159.

Santanello, J.A. and Co-authors (2018), Land–Atmosphere Interactions: The LoCo Perspective, *Bull. Amer. Meteor. Soc*, https://doi.org/10.1175/BAMS-D-17-0001.1.

Santanello, J.A.,, S.Q. Zhang, D.D. Turner, P. Lawston, and W.G. Blumberg, PBL Thermodynamic Profile Assimilation and Impacts on Land-Atmosphere Coupling, AGU Fall Meeting, San Francisco, CA, Dec. 9-13, 2019.

Tucker, S.C., S.J. Senff, A.M. Weickmann, W.A. Brewer, R.M. Banta, S.P. Sandberg, D.C. Law and R.M. Hardesty (2009), Doppler Lidar Estimation of Mixing Height Using Turbulence, Shear, and Aerosol Profiles, *J. Atmos. Ocean Tech.*, 26, 673-688.